The Crystal and Molecular Structures of Bigeranyl Tetrahydrochloride.
The Triclinic Modification*

By Frode Mo and Harald Sørum

Institute of X-ray Crystallography, The Technical University of Norway, Trondheim, Norway

Bigeranyl tetrahydrochloride (2,6,11,15-tetrachloro-2,6,11,15-tetramethylhexadecane, $C_{20}H_{38}Cl_4$), a lower homologue of squalene hexahydrochloride, is known to exhibit polymorphism. Spontaneous transition from the labile to the stable crystal form has been reported. The stable, triclinic modification, m.p. 110°C, crystallizes in space group $B\bar{1}$ ($Z=2$) with unit-cell parameters $a=20\cdot801$, $b=9\cdot743$, $c=6\cdot002$ Å; $\alpha=91\cdot3°$, $\alpha=91\cdot4°$, $\gamma=102\cdot8°$. Structure determination was initiated by means of the chlorine atoms. Positional parameters were first refined by the method of successive Fourier syntheses. Three-dimensional refinement was carried out with full-matrix least squares to a final discrepancy index, R_1, of 0·055. The molecules are mainly planar, centrosymmetric, and pack in layers parallel to (001). In the main molecular plane the carbon chains are bent at the central tertiary carbons thereby achieving a pronounced Z shape. The C–Cl bonds pointing out of this plane are unusually long: C(2)–Cl(1) $1\cdot856\pm0\cdot007$ Å and C(6)–Cl(2) $1\cdot858\pm0\cdot007$ Å. The main reason for this is believed to be short intramolecular Cl$\cdots$H approach distances. The Cl–C–C angles are in the range $105\cdot3-107\cdot6°\pm0\cdot4°$ which is less than the tetrahedral value.

Introduction

In the course of an investigation which led to the identification of the constitution of pristane, a saturated aliphatic hydrocarbon from the liver oil of the basking shark, N. A. Sørensen and his collaborators in 1947 synthesized as intermediates a new aliphatic diterpene, bigeranyl or 2,6,11,15-tetramethylhexadeca-2,6,10,14-tetraene, $C_{20}H_{34}$, and its crystalline tetrahydrochloride, $C_{20}H_{38}Cl_4$ (Sørensen & Mehlum, 1948; Sørensen, Gillebo, Holtermann & Sørensen, 1951). The diterpene was also later synthesized by Barnard & Bateman (1950). The tetrahydrochloride, which was prepared mainly as a means to purify the diterpene itself, was isolated as thin leaflets which after recrystallizations from ether melted at 110°C (Sørensen *et al.*, 1951). Sørum, Barstad & Dale (1956), hereafter SBD, later reported that bigeranyl tetrahydrochloride crystallizes in two modifications: thin plates of approximately hexagonal form melting at 95°C, and long needle-shaped crystals with m.p. 110°C. The lower-melting modification, crystallized from acetone, was found to be labile, being monotropically converted in the solid state to the stable, higher-melting modification. Crystals of the latter form may also be obtained by evaporation of a carbon disulfide solution. The authors' results from X-ray investigations as well as infrared spectroscopy provided clear evidence for the existence of two crystalline forms of the tetrahydrochloride, and even indicate, considering the morphological descriptions of the crystals, that the sample first isolated by Sørensen *et al.* was probably the lower-melting form. In a previous crystallographic investigation Sørum &

Dale (1955) had deduced the crystal structures of two modifications of squalene hexahydrochloride, $C_{30}H_{56}Cl_6$, from one-dimensional projections of the electron densities. Bigeranyl tetrahydrochloride is a lower homologue of this compound and preliminary crystal data for its two modifications have been given by SBD. The main purpose of this work was to establish the two crystal structures of bigeranyl tetrahydrochloride of which the stable, triclinic form will be reported here.

The phenomenon of polymorphism is frequently found in long carbon-chain compounds, and has been studied by means of X-ray methods in different groups of compounds, such as n-alkanes, fatty acids and esters, fatty alcohols, glycerides *etc.* If the structures of the polymorphic forms of bigeranyl tetrahydrochloride were determined, it should be possible to describe the rearrangements that must take place within the crystal cell during the transition from the labile to the stable phase. Also, it might be possible from the geometry and packing of the two polymorphs to come to conclusions concerning the nature of some of the major driving forces involved in the rearrangements. Both these points were thought to be of considerable interest from the outset of the work.

Experimental

Apparatus

A Siemens manual counter-tube goniometer with layer-line accessory for single-crystal examinations was employed; having a distance crystal–detector of 170 mm. No Eulerian cradle was available for the measurements. Diffracted intensities were both displayed as numbers of counts on an electronic panel (Siemens Type GS-DMZ) and given on a Kienzle printout.

Fairly good monochromatization was achieved by means of a $K\beta$ filter and a pulse-height discriminator. The X-ray tube voltage and current were stabilized by means of a Philips stabilizing unit PW1010/77. A scintillation counter [NaI(Tl) crystal] was used as a detector.

Crystal data

The crystals are colourless needles elongated parallel to [001]. A closer examination showed the forms {100} and {010} to be well developed.

Bigeranyl tetrahydrochloride, $C_{20}H_{38}Cl_4$
M.W. 419·95; m.p. 110°C .

Triclinic $a = 20\cdot801 \pm 0\cdot007$ Å; $\alpha = 91\cdot3° \pm 0\cdot1°$
$Z = 2$ $\quad b = 9\cdot743 \pm 0\cdot006$; $\beta = 91\cdot4 \pm 0\cdot1$
$\qquad c = 6\cdot002 \pm 0\cdot004$; $\gamma = 102\cdot8 \pm 0\cdot1$

Volume of the unit cell: $V = 1185$ Å³
Density, calculated (with $Z = 2$): $D_x = 1\cdot177$ g.cm⁻³; measured†: $D_m = 1\cdot19$ g.cm⁻³
Number of electrons per unit cell: $F(000) = 452$
Absorption coefficient for $\lambda_{Cu\ K\alpha}(= 1\cdot5418$ Å): $\mu = 45\cdot8$ cm⁻¹

Systematic absences: hkl when $(h + l)$ is odd corresponding to a base centring on (010).
Space group: $B\bar{1}$ a variant of C_i^1 .

The somewhat unusual choice of a base-centred triclinic cell was originally made in order to achieve a more direct comparison with the unit cell of the monoclinic form. Space group $B\bar{1}$ was strongly indicated on the basis of the statistical distribution of the $hk0$ intensities. The choice of $B\bar{1}$ was unequivocally confirmed during the refinement.

The specimen used for all measurements was a fragment of a larger crystal. Its cross-section as viewed along the needle axis can be described roughly as a parallelogram with edges $0\cdot39 \times 0\cdot24$ mm, but the regular outline was disrupted by a face which did not appear to be a characteristic one but rather a result of fragmentation of the larger crystal.

The agreement between the unit-cell data obtained in this work, and those reported by SBD is fairly good, except in the case of the angles α and α^*. The great differences between the α's and α^*'s may be explained, if one assumes that the SBD angle α^* actually is a misprint for $180° - \alpha^*$ (the SBD angle α^* being obtained from Weissenberg photographs).

Prior to the intensity measurements crystal and detector settings for the diffraction maxima were calculated with use of the unit-cell data obtained in this work, and good agreement was found with observed settings.

Intensity data

Intensities were measured with nickel-filtered copper radiation. Taking into account the doubly recorded intensities in Table 1 one finds that of 1311 indepen-

† Sørum, Barstad & Dale (1956).

dent reflexions, within the Cu $K\alpha$ sphere for the four layers considered, 1244 or 95% were measured. Two different counter techniques were employed to obtain the intensity data: All $hk0$ and $hk1$ reflexions were first recorded by the stationary-crystal stationary-counter method (Furnas, 1957). Later, some of the $hk0$ and $hk1$ reflexions together with all $hk2$ and $h0l$ reflexions were measured by the 2θ-scan technique (Furnas, 1957). The scanning range had to be varied from $\sim 1°$ for low-angle reflexions up to $\sim 6°$ for reflexions with 2θ near 160° to ensure complete registration of the $K\alpha_1$ and $K\alpha_2$ components. The detector aperture size was kept fixed at 2×2 mm² during the recordings which were made with a scanning rate of $1°.\text{min}^{-1}$. Intensity readings were corrected for background in the usual way. A manganese attenuator was used with the stronger reflexions to reduce counting errors.

Table 1. *Recorded integrated intensities*

In brackets are given, for the first 3 layers, the numbers of reflexions common to the $h0l$ layer (column 2) and the number actually observed twice (column 3).

Layer	Theoretically observable, N_T	Measured, N_M	N_M/N_T
$hk0$	264 (13)	249 (12)	94·5%
$hk1$	506 (26)	463 (26)	91·5
$hk2$	444 (23)	438 (23)	98·5
$h0l$	159	155	97·5
Total:	1373 (62)	1305 (61)	95·0

For each of the four groups of reflexions, $hk0$, $hk1$, $hk2$ and $h0l$, a special reflexion was selected as a standard. During the measurements in one particular group, the appropriate standard intensity was tested 2–3 times a day to make sure that all intensities in that group were on the same scale. Most of the reflexions common to both $h0l$ and the layers $hk(0-2)$ were measured twice (*cf.* Table 1). 94 $hk0$ reflexions, of which 19 had not been measured in the stationary series, and 93 $hk1$ reflexions were recorded by the 2θ-scan technique. Intensities from both series of measurements (I_s and $I_{2\theta}$) were compared graphically by plotting the ratio $I_{2\theta}/I_s$ against the reflecting angle (Mo, 1966). The result indicated that the stationary-counter technique, as applied to this particular crystal and with the chosen detector aperture width, implies a small but increasing loss of intensity with increase of angle 2θ from $2\theta \sim 40°$. The loss is, of course, mainly caused by the partial separation of the $K\alpha$ doublet and during the stationary series it was attempted to correct the intensities in the 2θ-range 70–120° for this error. Beyond $2\theta \sim 120°$ $K\alpha_1$ and $K\alpha_2$ were measured separately and their values added to give the total intensity. The graph showed, however, that serious errors were introduced in the I_s values in that range because the loss of counts due to the increasing broadening of the intensity peaks was neglected. All intensity values obtained in the stationary series were converted to 2θ-scan values, *i.e.* integrated intensities according to the intensity graphs,

and were used in the later stages of the work together with the integrated $hk2$ and $h0l$ intensities. The speed of collecting data by the stationary-crystal stationary-counter method does not remarkably exceed that of the 2θ-scan method.

Considering the dimensions of the crystal ($0.24 \times 0.39 \times 0.8$ mm³) and its linear absorption coefficient (45.8 cm⁻¹) for Cu $K\alpha$ radiation it was found necessary to correct the intensities for absorption. Because of the rather irregular shape of the crystal the corrections were made graphically using the principles of Albrecht (1939). The practical and rapid procedure invented by Rogers & Moffett (1956) was employed here directly for the $hk0$ intensities. By introducing certain modifications to account for the different geometry involved in the recording of higher-level intensities with the normal-beam technique, the same principle could be applied also to the $hk1$ and $hk2$ reflexions. All $hk0$ intensities and about 80% of the $hk1$ and $hk2$ intensities, totalling approximately 1000, were corrected for absorption in this way. The average number of sampling points per reflexion is estimated at 20-25. Transmission factors, T, for the remaining upper-level intensities were found by interpolation.

Correction of the $h0l$ intensities was carried out in an indirect manner by calculating appropriate T factors for the 61 doubly recorded $h0l$ reflexions when measured about the y axis. The reflecting position of the crystal and the directions of incoming and diffracted beams were drawn for each recording during these measurements. From a comparison of such

drawings, it was possible to estimate relative path lengths and values of T for the remaining reflexions in the $h0l$ zone. This process, which partly took on the character of an interpolation between previously calculated T factors, is believed to have given fairly reliable values.

The results from the graphical evaluation of transmission factors seem to justify the procedure. Thus, for instance, two of the 249 observed $hk0$ reflexions were found to have values of T as low as 0.21–0.22, while for eight others the T factors were in the range 0.42–0.47, which means that within the same level a few intensities were approximately twice as much reduced by absorption as others. About 65% of the $hk0$ reflexions had values of T in the range 0.32–0.37. A similar spread within the set of T factors was found also for the higher levels, the mean value for a level decreasing somewhat with increase of height over the equator, as expected. Lp corrections were made on a GIER computer using a modified program written by Borgen & Fremstad.

An approximate scale factor, K, for the observed F's and an isotropic temperature parameter, B, were found for the $hk0$ data by the method of Wilson (1942). The value of $K=2.76$ was refined successively while $B=3.9$ Å² was used unchanged for the individual atoms during the two-dimensional work.

Determination of the structure

A statistical analysis of the $hk0$ intensities (stationary series) was carried out according to the $N(z)$-test method of Howells, Phillips & Rogers (1950). The experimental distribution is clearly in favour of centrosymmetry in the projection along [001] as can be seen from Fig. 1. The heavy Cl atoms occupy general positions in the cell, so even if their contributions to the majority of the intensities were considerable, the interpretation of the experimental distribution should be quite safe; see also Howells, Phillips & Rogers (1950) and Sim (1958). Space group $B\bar{1}$ implies that there are 4 equivalent positions in the cell: x,y,z; $x+\frac{1}{2},y,z+\frac{1}{2}$; $\bar{x},\bar{y},\bar{z}$; $\bar{x}+\frac{1}{2},\bar{y},\bar{z}+\frac{1}{2}$. With $Z=2$ the molecules must be centrosymmetric, and the asymmetric unit contains two chlorine atoms.

Projection along [001]

A two-dimensional study was started as soon as the $hk0$ data from the stationary series were complete. The

heaviness index, defined as the ratio: $\overset{N}{\Sigma} Z_H^2 / \overset{n}{\Sigma} Z_L^2$, is 1.53 for this structure. Z_H and Z_L refer to the atomic numbers of the heavy and the light atoms, respectively (Mathieson, 1961). It seemed probable, therefore, that the chlorine atoms in the present case would dominate the majority of the phases, especially for the stronger F's, and interpretation of $P(xy)$ for the location of chlorine atoms was accordingly done as follows: In a projection along [001] of the cell outline a structure-
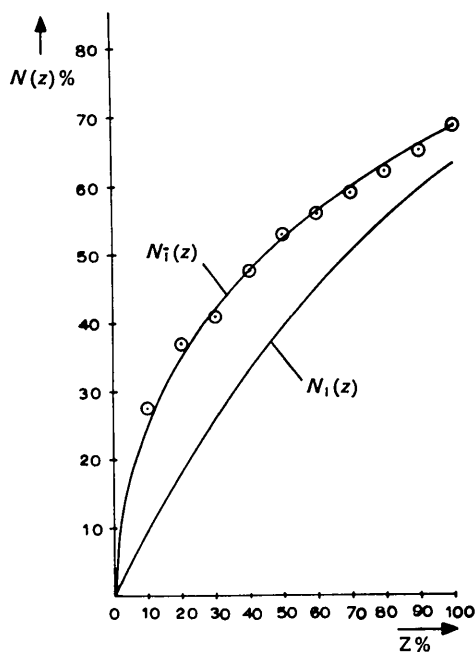

Fig. 1. Statistical distribution of intensities. Solid lines indicate theoretical distributions for acentric $[N_1(z)]$ and centric $[N_{\bar{1}}(z)]$ cases; circles with dots show calculated distribution of $hk0$ intensities.

factor map was prepared showing the traces of sets of planes corresponding to 8 strong $hk0$ reflexions, namely 020, 220, 400, $\overline{4}10$, $\overline{4}20$, 810, 1050 and $\overline{16}30$. Various arrangements of Cl were tested making use of the following criteria: a possible arrangement was expected both to give rise to recognizable maxima in the Patterson map and to contribute essentially, preferably to all the eight selected F_{hk0}'s.

Two different and acceptable Cl arrangements were found in this way and both were examined by calculating the corresponding sets of structure factors and discrepancy index $R_1 = \Sigma \, ||F_o| - |F_c||/\Sigma \, |F_o|$. One of the models had $R_1 \sim 0.63$ and was rejected, the other had $R_1 \sim 0.52$ and was investigated further. Estimated xy coordinates for the heavy atoms in the latter model were: 0·151, 0·298 and 0·395, 0·215.

184 F_o's were assumed to have signs controlled by the heavy atoms and were included in the calculation of the first density projection, $\varrho(xy)$. 167 of the signs were finally found to be correct, most of the included F_o's with wrong sign being weak. The first $\varrho(xy)$ map showed quite distinctly the carbon chains in addition to the chlorine atoms, and from a preliminary consideration of C–C distances in the map it became apparent that the molecule chains lie nearly parallel to (001). Thus, it was possible, already after the first calculation of $\varrho(xy)$, to assign approximate x and y coordinates to all carbon atoms in a molecule and refine the chlorine positions. The R_1 value for this structure model was 0·25.

Two successive Fourier summations were carried out, the second one with contributions only from the carbon atoms in order to obtain more exact positional parameters of the tertiary carbon atoms being masked

by the chlorine atoms in this projection. The corrections reduced R_1 to 0·174. At this stage 2θ-scan values for the 230 + 19 additional F_{hk0}'s were available. A second calculation of R_1 with the new set of F_o's resulted in a slight reduction to 0·171. Further refinement of the xy coordinates was deferred till the two-dimensional refinement of the [010] projection had been completed. Later, with x coordinates from the last $\varrho(xz)$ set, another density projection, $\varrho(xy)$, was computed with 238 terms. The resulting structure model had an R_1 index of 0·165. Fig.2 shows a projection of the electron density with a half molecule drawn in. The map has been prepared from parameters after the ultimate three-dimensional refinement.

Projection along [010]

The same method of interpretation as described for the [001] projection was tried also for a projection along [010]. The Patterson map, $P(xz)$, computed with 159 terms is shown in Fig.3(a). 8 sets of planes corresponding to some of the strongest $h0l$ reflexions were selected: 002, 101, 301, 400, $\overline{5}01$, $\overline{8}02$, 903 and $\overline{12}02$.

The two Cl atoms with coordinates $x = 0.152$ and $x = 0.106$ $(\tfrac{1}{2} - x)$ from the $\varrho(xy)$ refinement were considered first.

A model with the Cl pair placed nearly parallel to $(\overline{5}01)$ had an R_1 value of 0·51. For none of the other arrangements was R_1 below 0·63. Trial parameters of the best model were: 0·152, 0·858; 0·106, 0·658; the latter position is equivalent to 0·394, 0·842. Signs for the 8 strong F_{h0l}'s were given in accordance with the chlorine contribution and 125 terms were included in the computation of the first $\varrho(xz)$ projection. The signs of 114 of these were later found to be correct. In addi-
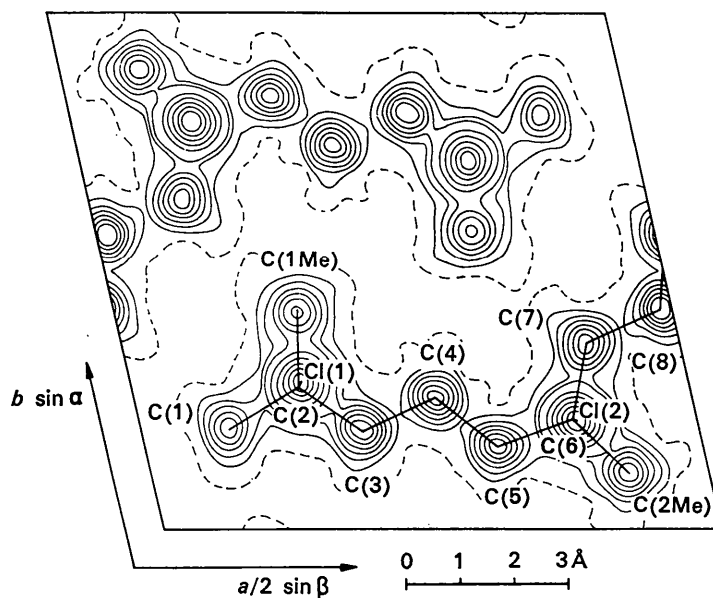

Fig.2. Final electron density projection $\varrho(xy)$. Contour lines are at intervals of 1 e.Å^{-2}, but around the chlorine positions the equidistance from the 4 e.Å^{-2} level is 4 e.Å^{-2}. The 1 e.Å^{-2} level line is broken.

tion to the chlorine positions the map (not reproduced) is dominated by two parallel density ridges at $z = \frac{1}{4}$ and $z = \frac{3}{4}$. All attempts to fit carbon atoms into the ridge at $z = \frac{1}{4}$ invariably resulted in an increase of R_1. Other Cl arrangements were now tested without much success. The first $\varrho(xz)$ map was then re-examined and a second start made by placing the four carbons C(2), C(5), C(6) and C(2Me) near $z = \frac{1}{2}$; x coordinates from the $\varrho(xy)$ refinement were used. Calculation of structure factors reduced R_1 to 0·46 and gave opposite signs for two reflexions: the very weak $\overline{9}05$ and the 002 'test reflexion' being the strongest of all in the $h0l$ zone. The density ridges in a second Fourier synthesis had moved to $z = 0$ and $z = \frac{1}{2}$, and carbon atoms C(1), C(3) and C(8) could also be identified. Based on known x coordinates it was possible, by the help of models, to assign approximate positions for all carbons in the chain. The corresponding R_1 value dropped to a convincing 0·215. Thus, the sign of the 002 reflexion turned out to be positive in spite of the sizable negative con-

tribution from the Cl atoms ($\frac{1}{4}$ of the total value), clearly demonstrating that the method of strongly reflecting planes, very efficient as it proved to be, has to be used with care.

Two-dimensional refinement was continued by means of two more Fourier syntheses, a difference synthesis followed by a final Fourier synthesis based on 152 terms. This gave a parameter set $[R_1(h0l) = 0·173]$ to be used for the three-dimensional refinement together with the last coordinates from the $\varrho(xy)$ refinement. The map in Fig. 3(b) was prepared after completion of the three-dimensional refinement. Structure factors and Fourier syntheses were computed on GIER using modified versions of programs devised by Borgen & Fremstad.

Three-dimensional refinement

Three-dimensional refinement was carried out mainly by the method of least-squares using the program LSFIV 2 by Borgen & Mestvedt (1966a). This is a full-
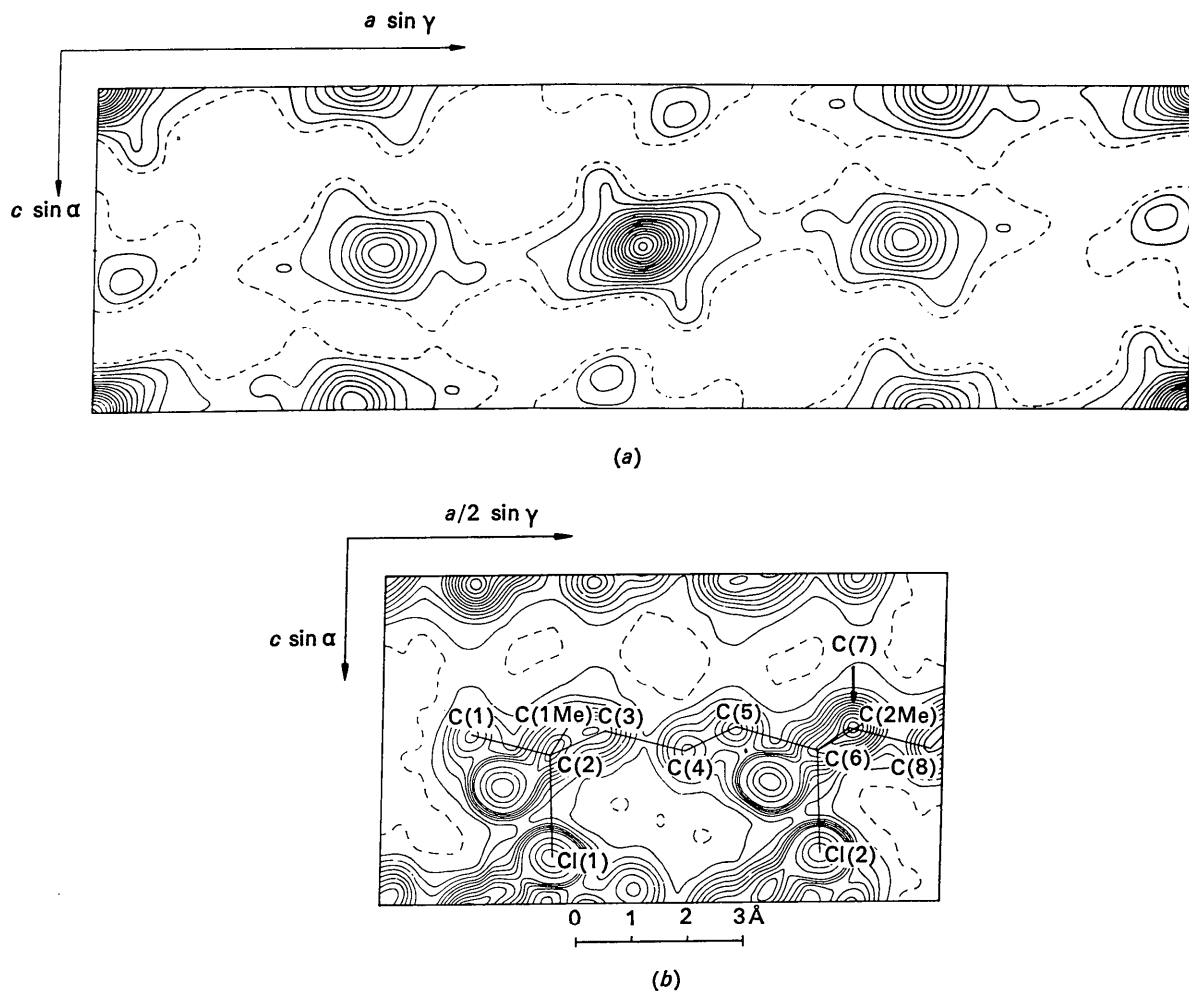

(a)

(b)

Fig. 3. (a) Patterson projection $P(xz)$. Contour lines are at arbitrary but equal intervals. Zero level line is broken. (b) Final electron density projection $\varrho(xz)$. Contour lines are at intervals of 1 e.Å^{-2}, but around the chlorine positions the equidistance from the 8 e.Å^{-2} level is 4 e.Å^{-2}. The 1 e.Å^{-2} level line is broken.

matrix program minimizing $\Sigma w(|F_o| - |F_c|)^2$ and is based on the program ORFLS by Busing, Martin & Levy (1962). Two difference syntheses were computed in order to obtain hydrogen coordinates. Program FOUAL 3 (Borgen & Mestvedt, 1966b) was employed for this purpose. Atomic scattering factors for Cl, C and H as given in *International Tables for X-ray Crystallography* (1962) were used. All computations were carried out on a UNIVAC 1107. Scale factors for the layers $hk0$, $hk1$, $hk2$ and $h0l$ were refined individually in the least-squares cycles. All observed structure factors were given unit weight. The process of refinement, which proceeded rapidly, is presented briefly in Table 2. Isotropic temperature factors of the heavier atoms (Cl and C) were refined before conversion to anisotropic form after cycle 5. In order to prevent possible interaction between shifts in β_{33}'s and in scale factors the latter were kept constant in cycles 6–7. Subsequent refinement of scale factors as well caused only small parameter shifts.

From the first difference map after cycle 9, approximate positions of the 19 hydrogen atoms were easily recognized at the centres of peaks of density 0·15–0·5 e.Å^{-3}. Two or three of the derived positions indicated rather too long C–H bonds, but they were used unaltered for the calculation of structure factors prior to cycle 10. Each hydrogen atom was then arbitrarily assigned an isotropic thermal parameter 1·5 Å^2 greater than that found after cycle 5 for the carbon atom to which it is attached. This gave values of B for hydrogen ranging from 5·1 to 6·8 Å^2. All hydrogen parameters were kept fixed in cycle 10. The hydrogen maxima in the second difference map appeared rounder and more distinct and were of density 0·27–0·54 e.Å^{-3}. There were no other regions of appreciable electron density. An attempt to refine hydrogen coordinates and temperature parameters, following cycle 11, resulted in a considerable decrease in B for nearly all hydrogen atoms. Only coordinates were refined in cycles 12–13, and then the hydrogen atoms had been assigned a B of 3·5 Å^2 which was assumed to be a better approxima-

tion. The assumption was confirmed by the small but significant reduction of R_1 before cycle 12 (see also *Discussion*). Two near-zero reflexions, $\overline{1}03$ and $\overline{12},11,2$, being obviously in error, were removed from the data list during the later stages of refinement. Two of the last coordinate shifts of the heavier atoms were as large as one-tenth of the e.s.d. of atomic positions; the others were less. Final thermal parameter shifts of the heavier atoms were of magnitude one-quarter of the e.s.d. of the parameters or less. None of the last coordinate shifts of the hydrogen atoms exceeded $\frac{1}{2}$ of the corresponding e.s.d.'s.
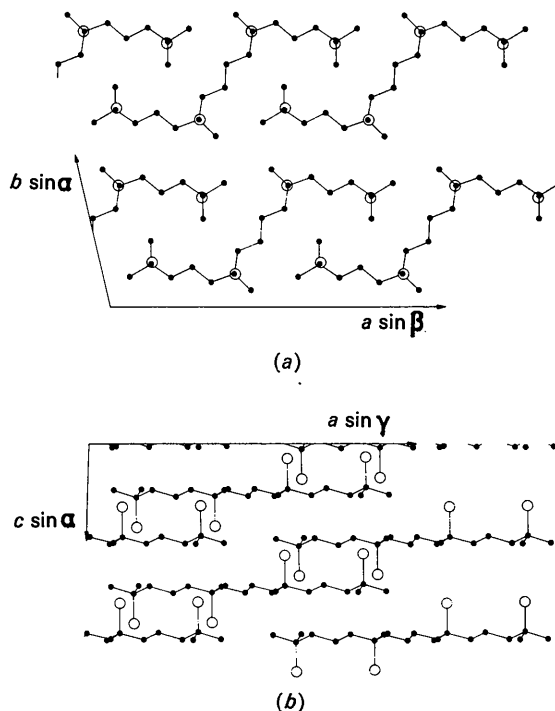

Fig. 4. Packing of the molecules as viewed down the z axis (a) and the y axis (b). In both (a) and (b) open and filled circles are chlorine and carbon atoms, respectively.

Table 2. *Progress of three-dimensional refinement*

XYZ and xyz denote coordinates of heavier atoms and hydrogen atoms, respectively; B and β_{ij} are isotropic and anisotropic thermal parameters of heavier atoms, respectively. B_H's are isotropic thermal parameters of hydrogen atoms, and S_q's are scale factors.

Calculation	Refining or determining	R_1	Remarks
LS cycles 1–2	S_q, XYZ	0·246–0·207	
LS 3–5	S_q, XYZ, B	0·207–0·130	
LS 6–7	XYZ, β_{ij}	0·130–0·108	Anisotropic refinement begun.
LS 8–9	S_q, XYZ, β_{ij}	0·108–0·108	
3–D diff. map 1.	xyz		H peaks of 0·15–0·5 e.Å^{-3}
LS 10	S_q, XYZ, β_{ij}	0·083–0·068	H included in F_c
Structure factors		0·105	H not included
3–D diff. map 2.	xyz		H peaks of 0·27–0·54 e.Å^{-3}
LS 11	S_q, XYZ, β_{ij}	0·066–0·064	H included in F_c
LS 12–13	S_q, xyz	0·062–0·059	Used value of $B_H = 3·5$ Å^2
LS 14–15	S_q, xyz, B_H	0·059–0·058	
LS 16–17	S_q, XYZ, β_{ij}	0·058–0·056	
LS 18–19	S_q, xyz, B_H	0·056–0·055	Final refinement and calc. of 1242 F's.

Averaged e.s.d.'s of atomic coordinates are:

Cl $\sigma(x) \sim \sigma(y) = 0.0012$ Å , $\sigma(z) = 0.0017$ Å ;
C $\sigma(x) \sim \sigma(y) = 0.0038$ Å , $\sigma(z) = 0.0058$ Å ;
H $\sigma(x) \sim \sigma(y) = 0.04$ Å , $\sigma(z) = 0.045$ Å .

Final positional and thermal parameters are given in Tables 3, 4 and 5. Final values of scale factors for the layers $hk0$, $hk1$, $hk2$ and $h0l$ were: 2·85, 2·91, 2·91 and 3·07, respectively. Program LSFIV 2 also computes the weighted discrepancy index $R_2 = [\Sigma w(|F_o| - |F_c|)^2 / \Sigma w \cdot F_0^2]^{\frac{1}{2}}$ ($w = 1$ here). The ultimate values are given below:

R_1 including zero obs.: 0·055 ;
R_2 including zero obs.: 0·048 ;
R_1 omitting zero obs.: 0·051 ;
R_2 omitting zero obs.: 0·045 .

A complete list of observed and calculated structure factors may be obtained from the authors.

Table 3. Final coordinates of the heavier atoms

Standard deviations ($\times 10^5$) appear in brackets.

	x	y	z
Cl(1)	0·1533 (6)	0·2874 (13)	0·8613 (29)
Cl(2)	0·3925 (5)	0·2110 (12)	0·8513 (29)
C(1)	0·0785 (19)	0·1941 (50)	0·4893 (104)
C(2)	0·1495 (18)	0·2754 (40)	0·5520 (116)
C(3)	0·1982 (17)	0·1897 (37)	0·4801 (85)
C(4)	0·2702 (17)	0·2557 (39)	0·5419 (91)
C(5)	0·3157 (17)	0·1603 (37)	0·4695 (87)
C(6)	0·3891 (17)	0·2123 (36)	0·5418 (110)
C(7)	0·4167 (17)	0·3621 (37)	0·4746 (88)
C(8)	0·4894 (17)	0·4242 (36)	0·5387 (90)
C(1Me)	0·1644 (23)	0·4260 (44)	0·4713 (112)
C(2Me)	0·4284 (18)	0·1080 (39)	0·4639 (93)

Discussion of the structure

Fig. 4 shows the molecular packing arrangement. The carbon chains appear planar in the projection along [010] [Fig. 4(b)] and form layers parallel to (001). The two chlorine atoms of one half-molecule are situated on the same side of the main molecular plane, the di-

Table 5. Final parameters of the hydrogen atoms

Standard deviations of coordinates ($\times 10^3$) appear in brackets. The first number (and letters) in brackets refer to the number of the carbon atom to which the hydrogen atom is bonded.

	x	y	z	B
H(11)	0·048 (2)	0·242 (4)	0·553 (8)	2·4 Å^2
H(12)	0·070 (2)	0·083 (4)	0·529 (8)	3·6
H(13)	0·077 (2)	0·201 (4)	0·367 (9)	4·4
H(31)	0·184 (1)	0·093 (3)	0·550 (7)	1·8
H(32)	0·194 (2)	0·191 (4)	0·326 (7)	2·4
H(41)	0·269 (2)	0·265 (4)	0·692 (8)	3·5
H(42)	0·284 (1)	0·357 (3)	0·469 (7)	1·4
H(51)	0·298 (2)	0·057 (4)	0·540 (7)	2·0
H(52)	0·316 (2)	0·147 (4)	0·320 (8)	2·9
H(71)	0·389 (1)	0·429 (3)	0·541 (7)	0·9
H(72)	0·415 (2)	0·366 (4)	0·343 (8)	3·1
H(81)	0·492 (2)	0·437 (4)	0·751 (8)	4·4
H(82)	0·517 (1)	0·367 (3)	0·496 (7)	0·8
H(1Me1)	0·132 (2)	0·477 (4)	0·543 (8)	3·0
H(1Me2)	0·153 (2)	0·404 (5)	0·379 (9)	6·5
H(1Me3)	0·204 (2)	0·469 (5)	0·495 (9)	5·2
H(2Me1)	0·407 (1)	0·013 (3)	0·511 (7)	1·5
H(2Me2)	0·428 (2)	0·112 (4)	0·286 (8)	3·3
H(2Me3)	0·468 (1)	0·128 (3)	0·515 (7)	1·5

rection of the C–Cl bonds being very nearly parallel to the z axis.

Superposed on the usual carbon-chain zigzag pattern in the main plane of the molecule [Fig. 4(a)] there is a bend at the tetrasubstituted carbons. The molecules thereby achieve a characteristic Z shape. The bending is thought to be mainly due to steric interaction between methylene groups in the chain and the bulky methyl groups and conforms well with what has been found for similar structures. Abrahamsson & Westerdahl (1963) have pointed out that bending is a common feature in long-chain molecules where the hydrocarbon chain packing is disturbed by the presence of groups other than methylene groups along the molecule. The angle of bend, $\angle$C(2)–C(6)–C(6'), is $115.0° \pm 0.1°$ (primes are used for centrosymmetrically related atoms of the same molecule).

A more precise description of the carbon arrangement within the main molecular plane would be as follows: The carbon atoms constituting one wing of

Table 4. Final thermal parameters, β_{ij} ($\times 10^4$), of the heavier atoms

β as given here is defined by:

$$\exp [-(h^2\beta_{11} + k^2\beta_{22} + l^2\beta_{33} + 2hk\beta_{12} + 2hl\beta_{13} + 2kl\beta_{23})].$$

Standard deviations ($\times 10^4$) appear in brackets. For explanation of B, see text.

	β_{11}	β_{22}	β_{33}	β_{12}	β_{13}	β_{23}	B_{11}	B_{22}	B_{33}
Cl(1)	34 (0)	182 (2)	282 (7)	21 (1)	7 (1)	−3 (4)	5·62 Å^2	6·55 Å^2	4·05 Å^2
Cl(2)	32 (0)	148 (1)	275 (7)	9 (1)	−2 (1)	34 (4)	5·29	5·34	3·96
C(1)	21 (1)	187 (7)	535 (33)	17 (2)	−14 (4)	−27 (12)	3·51	6·74	7·69
C(2)	23 (1)	114 (5)	351 (28)	13 (2)	−16 (4)	−29 (12)	3·78	4·13	5·06
C(3)	20 (1)	107 (4)	270 (22)	7 (2)	−7 (4)	−1 (9)	3·37	3·84	3·89
C(4)	20 (1)	113 (4)	398 (27)	8 (2)	3 (4)	−33 (10)	3·28	4·08	5·73
C(5)	22 (1)	102 (4)	313 (23)	6 (2)	−3 (4)	−24 (9)	3·62	3·69	4·50
C(6)	21 (1)	92 (4)	291 (25)	10 (2)	−3 (4)	−3 (11)	3·53	3·30	4·18
C(7)	21 (1)	98 (4)	291 (28)	8 (2)	6 (4)	32 (9)	3·41	3·54	4·19
C(8)	20 (1)	102 (4)	366 (29)	7 (2)	4 (4)	39 (9)	3·24	3·69	5·27
C(1Me)	37 (1)	116 (5)	632 (41)	22 (2)	−9 (6)	5 (11)	6·09	4·18	9·09
C(2Me)	26 (1)	110 (4)	357 (31)	18 (2)	6 (4)	−4 (10)	4·25	3·95	5·14

the molecule, *viz.* C(1), C(2), C(3), C(4), C(5) and C(6)+C(2Me) lie very nearly in a plane which is, of course, parallel to the plane-defining atoms C(1'), C(2'), C(3'), C(4'), C(5') and C(6')+C(2'Me). Carbon atoms C(5), C(6), C(7), C(8), C(8'), C(7'), C(6') and C(5') are nearly contained within another plane twisted by about 51° with respect to the planes of the wings, the angle being defined as the angle between the plane normals. In the asymmetric unit carbon atoms C(4), C(5), C(6) and C(7) thereby conform to the favourable cyclohexane chair arrangement in which C(3), C(2Me) and C(8) are equatorial substituents and Cl(2) is axial substituent. The central four carbon atoms of each molecule lie in a plane which make an angle of about 44° with the *y* axis.

Bond lengths and bond angles have been computed by means of program PAFIV 1 (Borgen & Mestvedt, 1966c) which is based on program ORFFE by Busing, Martin & Levy (1964). The values are given in Tables 6 and 7. Allowance for errors in the unit-cell parameters has been made in the listed e.s.d.'s. Interatomic distances have not been corrected for the effect of thermal motion of the individual atoms.

Table 6. *Bond lengths*

Standard deviations ($\times 10^3$) of bonds between heavier atoms appear in brackets.

C(2)–Cl(1)	1·856 (7) Å	C(1)——H(11)	0·94 Å
C(6)–Cl(2)	1·858 (7)	C(1)——H(12)	1·09
C(1)–C(2)	1·546 (7)	C(1)——H(13)	0·74
C(2)–C(1Me)	1·524 (7)	C(3)——H(31)	1·02
C(2)–C(3)	1·513 (6)	C(3)——H(32)	0·93
C(3)–C(4)	1·526 (6)	C(4)——H(41)	0·90
C(4)–C(5)	1·530 (6)	C(4)——H(42)	1·06
C(5)–C(6)	1·546 (6)	C(5)——H(51)	1·09
C(6)–C(7)	1·513 (6)	C(5)——H(52)	0·90
C(6)–C(2Me)	1·512 (6)	C(7)——H(71)	1·05
C(7)–C(8)	1·535 (6)	C(7)——H(72)	0·79
C(8)–C(8')	1·531 (7)	C(8)——H(81)	1·27
		C(8)——H(82)	0·92
		C(1Me)–H(1Me1)	1·02
		C(1Me)–H(1Me2)	0·61
		C(1Me)–H(1Me3)	0·84
		C(2Me)–H(2Me1)	0·99
		C(2Me)–H(2Me2)	1·07
		C(2Me)–H(2Me3)	0·86

All valence angles about the C–Cl bonds fall in the range 105·3–107·6° [$\sigma(\psi)=0·4°$] thus being less than the tetrahedral value. The C–C–C angles along the

Table 7. *Bond angles*

Standard deviations appear in brackets.

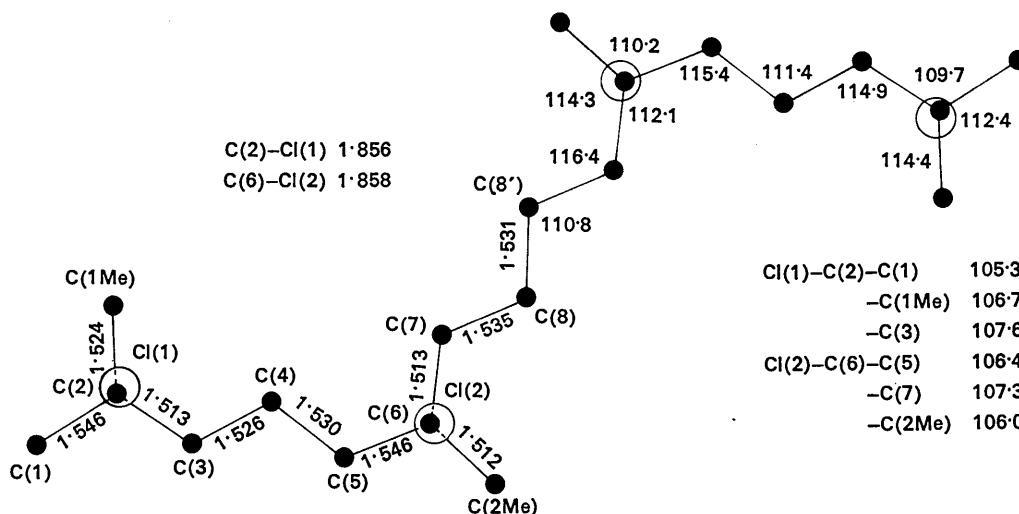|	ψ		ψ
Cl(1)——C(2)–C(1)	105·3 (0·4)°	C(2)–C(3)–C(4)	114·9 (0·4)°
–C(1Me)	106·7 (0·4)	C(3)–C(4)–C(5)	111·4 (0·4)
–C(3)	107·6 (0·4)	C(4)–C(5)–C(6)	115·4 (0·4)
Cl(2)——C(6)–C(5)	106·4 (0·4)	C(5)–C(6)–C(7)	112·1 (0·4)
–C(7)	107·3 (0·4)	–C(2Me)	110·2 (0·4)
–C(2Me)	106·0 (0·4)	C(7)–C(6)–C(2Me)	114·3 (0·4)
C(1)——C(2)–C(1Me)	112·4 (0·5)	C(6)–C(7)–C(8)	116·4 (0·4)
–C(3)	109·7 (0·4)	C(7)–C(8)–C(8')	110·8 (0·5)
C(1Me)–C(2)–C(3)	114·4 (0·5)		

Fig. 5. Bond lengths (Å) and bond angles (°). Open and filled circles are chlorine and carbon atoms respectively. The atomic numbering used is indicated.

chain range from 109·7° to 116·4° [$\sigma(\psi) = 0$·4–0·5°] which agrees well with data reported on many other carbon-chain compounds. It will be noticed that all the larger angles, *viz.* C(1Me)–C(2)–C(3) (114·4°), C(2)–C(3)–C(4) (114·9°), C(4)–C(5)–C(6) (115·4°), C(7)–C(6)–C(2Me) (114·3°), C(6)–C(7)–C(8) (116·4°) effect lengthening of short intramolecular hydrogen contacts either with the Cl atoms or with 1 Me or 2 Me.

The C–Cl bonds are remarkably long. The average C–Cl distance from the two bond lengths found in this work is 1·857 ± 0·007 Å. Values reported in the literature seem to indicate that a 'normal' aliphatic C–Cl bond is about 1·78–1·79 Å. Altona, Knobler & Romers (1963) have listed some bond lengths of this type obtained from electron-diffraction experiments (E.D.) or microwave spectroscopy (M.S.). Of greater interest in the present case is probably the C–Cl distance found in t-butyl chloride, in which the chlorine atom is bonded to a tertiary carbon atom: 1·768 Å (E.D.) (Bowen, Gilchrist & Sutton, 1955), whereas Coutts & Livingston (1953) report 1·80 Å (E.D.). According to Coutts & Livingston the Cl–C–C angle in this molecule is 107·5°, *i.e.* significantly less than 109·5°. Longer C–Cl bonds have been reported for other types of compound. A few examples will be given: 1-chlorobut-2-yne, 1·798 Å (M.S.) (Laurie & Lide, 1959); acetyl chloride, 1·82 (E.D.) (Allen & Sutton, 1951) and allyl chloride, 1·825 Å (E.D.) (Bowen, Gilchrist & Sutton, 1955). X-ray determinations of C–Cl bond lengths in compounds in the solid state have given even higher values. Altona, Knobler & Romers (1963) found a bond length of 1·845 Å in *trans*-2,5-dichloro-1,4-dioxane at −125°C and a more recent crystal-structure determination of 2β,3α-dichloro-5α-cholestane at −120°C by Geise, Romers & Rutten (1966) gave C–Cl distances of 1·80 and 1·82 Å.

In their discussion of the structures of the allyl halides and t-butyl halides Bowen *et al.* (1955) observe that the length of a C–Hal bond appears to be an inverse measure of its intrinsic strength. The relatively long C–Cl distances in compounds like 1-chlorobut-2-yne and acetyl chloride in which the chlorine atoms are more reactive than in compounds with 'normal' aliphatic C–Cl bonds may be said to support this view. The chlorine atoms in *trans*-2,5-dichloro-1,4-dioxane are also highly reactive, for instance in hydrolysis reactions, and Altona *et al.* (1963) have explained the presence of the unusual C–Cl distances along similar lines. It may be well worth observing, however, that measurements of the dipole moment of the likewise highly reactive monochlorodioxane did not indicate that the C–Cl bonds are ionized to any appreciable extent. This is consistent with dipole-moment data obtained by Allen & Sutton (1951) for the acetyl halides. Altona *et al.* (1963) *inter alia* point out that the spatial arrangement of atoms and lone-electron pairs may also be of importance in this connexion, but state that a fully satisfactory explanation of the phenomenon cannot be given.

In the present case the chlorine atoms must be characterized as relatively unreactive, *cf.* the observation by Sørensen *et al.* (1951) on the regeneration of bigeranyl from the tetrahydrochloride. Therefore, reactivity does not seem to account adequately for the long C–Cl bonds in bigeranyl tetrahydrochloride. Now, the above-mentioned relation between bond length and bond strength was developed for compounds in the gaseous phase. It appears likely that other factors, such as molecular packing geometry and approach distances, may exert a stronger influence on C–Hal bond lengths in solid-state compounds. In bigeranyl tetrahydrochloride the axial chlorine atoms will interact with neighbouring hydrogen atoms, both axial and equatorial, in the same molecule. A tentative, but qualitative, explanation in this case is that the increase of C–Cl distances is effected by the relatively short intramolecular Cl···H contacts, some of which are listed in Table 8.

Table 8. *Some intra- and intermolecular* Cl···H *approach distances*

I x, y, z; II $1-x, 1-y, 1-z$;
III $\tfrac{1}{2}+x, y, \tfrac{1}{2}+z$; IV $\tfrac{1}{2}-x, 1-y, \tfrac{3}{2}-z$

Cl	H	Cl···H
Cl(1)(I)	H(11)(I)	2·78 Å
	H(1Me1)(I)	2·78
	H(31)(I)	2·81
	H(41)(I)	2·69
	H(71)(IV)	3·12
	H(2Me1)(IV at $X, Y-1, Z$)	3·04
	H(32)(I at $X, Y, Z+1$)	3·12
Cl(2)(I)	H(41)(I)	2·87
	H(51)(I)	2·82
	H(71)(I)	2·87
	H(81)(I)	2·75
	H(2Me1)(I)	2·84
	H(2Me3)(I)	2·80
	H(31)(IV at $X, Y-1, Z$)	3·12
	H(2Me2)(I at $X, Y, Z+1$)	2·94

The C–C bonds range from 1·512 to 1·546 Å with an average e.s.d. of 0·006 Å. The average bond length between methylene carbon atoms, *viz.* C(3)–C(4), C(4)–C(5), C(7)–C(8) and C(8)–C(8′), is 1·531 ± 0·006Å, which may be compared with the value 1·533 ± 0·003 Å reported for the n-alkanes (Bartell, 1959). Lide (1962) reports 1·526 Å for the C(sp^3)–C(sp^3) bond, whereas Bastiansen & Trætteberg (1962) gives 1·534 Å for this bond. The average of all C–C bonds from this work is 1·528 ± 0·006 Å. All C–C bond lengths obtained may be considered normal and deserve no further comments.

The 19 C–H bond lengths listed in Table 6 are seen to vary considerably. E.s.d.'s have not been calculated, but the error is assumed to be in the range 0·05–0·10 Å. Except for the bond C(8)–H(81) all bonds between chain carbon and hydrogen atoms out of the main

molecular plane are shorter than those lying more or less in this plane. The average length of all in-plane (equatorial) C–H bonds is 0·99 Å; the corresponding out-of-plane (axial) value [omitting C(8)–H(81)] is 0·85 Å. The temperature factors of the axial hydrogen atoms appear to be larger than those of the equatorial hydrogen atoms. As would be expected, hydrogen atoms bonded to terminal carbon atoms C(1) and C(1Me) have comparably large B values.

The β_{ij}'s of the heavier atoms have been converted to B_{ii}'s or radii of the thermal vibration ellipsoids along the three principal reciprocal axes according to the relations $\beta_{11} = B_{11} \cdot a^{*2}/4$, etc., and the results are given in Table 4. Comparison of values in Tables 4 and 5 show that the B's of the hydrogen atoms are generally less than the averaged B_{ii}'s of the carbon atoms to which they are bonded. The opposite result would be expected. Similar findings apparently are not unusual in present-day crystal-structure determinations; see e.g. High & Kraut (1966) and Hanson (1966). Jensen & Sundaralingam (1964) have discussed this anomaly and ascribe it to the use of an inappropriate scattering-factor curve for hydrogen. The results indicate that the electron cloud in a bonded hydrogen atom is more localized than in the free atom and the small values of B factors, which even may come out negative (cf. Hanson, 1966; Hirshfeld, Sandler & Schmidt, 1963), may be looked upon as a compensation for errors introduced by the use of a non-bonded atom model for the calculation of hydrogen scattering factors. New scattering factors calculated by Stewart, Davidson & Simpson (1965) appear to be a better approximation.

Intra- and intermolecular atomic distances up to 4·2 Å have been exhaustively calculated. For the present discussion coordinate sets of the 4 asymmetric units, denoted by Roman numerals I to IV, have been rewritten as follows: I x,y,z; II $1-x,1-y,1-z$; III $\frac{1}{2}+x,y,\frac{1}{2}+z$; IV $\frac{1}{2}-x,1-y,\frac{3}{2}-z$.

All Cl···Cl approach distances are greater than 4·2 Å. Only four Cl···C intermolecular distances are less than 4·0 Å, the shortest being: Cl(1)(I)···C(1Me) (I at $X,Y,Z+1$) = 3·87 Å and Cl(2)(I)···C(2Me) (I at $X,Y,Z+1$) = 3·94 Å. The shortest intermolecular C···C contacts are: C(1)(I)···C(2Me) (IV at $X,Y-1,Z-1$) = 3·94 Å and C(1Me)(I)···C(7) (IV at $X,Y,Z-1$) = 3·99 Å. Cl···H approach distances appear to be more important for the molecular packing. The shortest of them are listed in Table 8. Some of the intramolecular possible weak Cl···H bonds are rather short compared with the effective van der Waals radii of the participants, i.e. Cl = 1·8 Å and H = 1·0–1·4 Å, and it is believed that they may be the main cause of the observed increase of C–Cl bond lengths.

The shortest C···H contact is C(1)(I)···H(2Me2) (IV at $X,Y-1,Z-1$) = 3·35 Å. There are about ten others in the range 3·46–3·60 Å. Only four H···H intermolecular distances fall below 3·0 Å. They are: H(12)(I)···H(2Me2) (IV at $X,Y-1,Z-1$) = 2·66 Å;

H(1Me1)(I)···H(71) (IV) = 2·72 Å; H(2Me2)(I)··· H(11) (III at $X,Y,Z-1$) = 2·94 Å and H(31)(I)··· H(51) (IV at $X,Y-1,Z$) = 2·95 Å.

References

ABRAHAMSSON, S. & WESTERDAHL, A. (1963). Acta Cryst. 16, 404.
ALBRECHT, G. (1939). Rev. Sci. Instrum. 10, 221.
ALLEN, P. W. & SUTTON, L. E. (1951). Trans. Faraday Soc. 47, 236.
ALTONA, C., KNOBLER, C. & ROMERS, C. (1963). Acta Cryst. 16, 1217.
BARNARD, D. & BATEMAN, L. (1950). J. Chem. Soc. p. 932.
BARTELL, L. S. (1959). J. Amer. Chem. Soc. 81, 3497.
BASTIANSEN, O. & TRÆTTEBERG, M. (1962). Tetrahedron, 17, 147.
BORGEN, O. & MESTVEDT, B. (1966a). Technical Report 38, Inst. of Phys. Chem., NTH.
BORGEN, O. & MESTVEDT, B. (1966b). Technical Report 46, Inst. of Phys. Chem., NTH.
BORGEN, O. & MESTVEDT, B. (1966c). Technical Report 47, Inst. of Phys. Chem., NTH.
BOWEN, H. J. M., GILCHRIST, A. & SUTTON, L. E. (1955). Trans. Faraday Soc. 51, 1341.
BUSING, W. R., MARTIN, K. O. & LEVY, H. A. (1962). OR FLS, A FORTRAN Crystallographic Least-Squares Program. U.S. Atomic Energy Commission Publication ORNL–TM-305.
BUSING, W. R., MARTIN, K. O. & LEVY, H. A. (1964). OR FFE, A FORTRAN Crystallographic Function and Error Program. U.S. Atomic Energy Commission Publication ORNL–TM–306.
COUTTS, J. W. & LIVINGSTON, R. L. (1953). J. Amer. Chem. Soc. 75, 1542.
FURNAS, T. C., JR (1957). Single Crystal Orienter Instruction Manual. Milwaukee: General Electric Company.
GEISE, H. J., ROMERS, C. & RUTTEN, E. W. M. (1966). Acta Cryst. 20, 249.
HANSON, A. W. (1966). Acta Cryst. 21, 97.
HIGH, D. F. & KRAUT, J. (1966). Acta Cryst. 21, 88.
HIRSHFELD, F. L., SANDLER, S. & SCHMIDT, G. M. J. (1963). J. Chem. Soc. p. 2108.
HOWELLS, E. R., PHILLIPS, D. C. & ROGERS, D. (1950). Acta Cryst. 3, 210.
International Tables for X-ray Crystallography (1962). Vol. III, p. 202. Birmingham: The Kynoch Press.
JENSEN, L. H. & SUNDARALINGAM, M. (1964). Science, 145, 1185.
LAURIE, V. W. & LIDE, JR., D. R. (1959). J. Chem. Phys. 31, 939.

LIDE, JR., D. R. (1962). *Tetrahedron,* **17**, 125.
MATHIESON, A. MCL. (1961). *Pure and Appl. Chem.* **2**, 505.
MO, F. (1966). Thesis, The Technical Univ. of Norway, Trondheim.
ROGERS, D. & MOFFETT, R. H. (1956). *Acta Cryst.* **9**, 1037.
SIM, G. A. (1958). *Acta Cryst.* **11**, 420.
STEWART, R. F., DAVIDSON, E. R. & SIMPSON, W. T. (1965). *J. Chem. Phys.* **42**, 3175.

SØRENSEN, N. A., GILLEBO, T., HOLTERMANN, H. & SØREN-SEN, J. S. (1951). *Acta Chem. Scand.* **5**, 757.
SØRENSEN, N. A. & MEHLUM, J. (1948). *Acta Chem. Scand.* **2**, 140.
SØRUM, H., BARSTAD, J. & DALE, J. (1956). *Acta Chem. Scand.* **10**, 1663.
SØRUM, H. & DALE, J. (1955). *Acta Chem. Scand.* **9**, 141.
WILSON, A. J. C. (1942). *Nature, Lond.* **150**, 151.

The Crystal and Molecular Structure of Cyclotetratriacontane [CH$_2$]$_{34}$

BY H.F. KAY AND B.A. NEWMAN*

H.H.Wills Physics Laboratory, Bristol University, England

Crystals of cyclic paraffins of long chain lengths have considerable interest in relation to the chain-folded nature of the crystallization of polymers in general. A three-dimensional analysis of [CH$_2$]$_{34}$ crystals indicates that the molecular rings are collapsed and are basically in the form of two roughly parallel zigzag chains of 15 atoms, linked at each end by two closure atoms, and conforming to a path traceable in the diamond structure. Small twists and bond distortions occur in the side chains as a result of steric hindrance at the closure atoms, which hindrance is also indicated by extensive strain at the molecule ends. The sub-cell is described in detail and related to other polymeric materials. A final *R* value of 0·16 was achieved with the use of 446 reflexion intensities.

Introduction

In recent years, the preparation of single crystals of a number of different polymers has been reported, for example, polyethylene (Keller, 1957; Fischer, 1957; Till, 1957), polyoxymethylene (Geil, 1960), cellulose (Manley, 1961), polypropylene (Morrow, Sauer & Woodward, 1965), establishing beyond doubt the general occurrence of the single-crystal phase in polymers. Such crystallization takes place by a folding of the main polymer chains at regular intervals, the distance between successive folds (the fold length) being constant for crystals prepared at a particular temperature. The crystals are thin platelets, the thickness being usually equal to one or a few of the fold lengths which are ~100 Å each. Such crystals are well suited for study by the electron microscope, investigations with which have revealed a wealth of morphological detail. The extreme fragility of these crystals has limited X-ray study to the more robust aggregates, and up to the present, the arrangement of atoms in the folded regions and the influence of this, if any, on polymer properties has not been established.

There is another class of compound in which sharp folds occur between carbon chains; this is the homologous series of large cyclic paraffins [CH$_2$]$_n$ first prepared by Ruzicka, Plattner & Wild (1964). The work

of Ruzicka and co-workers, combined with the X-ray observations of Muller (1933), established that the large rings ($n > 22$) crystallized as two parallel linear chains, linked by a few closure atoms at either end.

It was considered that an X-ray analysis of the crystal structures of cyclic paraffins would be useful, in order to reveal features that might be applicable to polyethylene. With the same chain packing, the same fold configuration would be anticipated. It can be supposed that several fold configurations are possible for cyclic paraffins, depending on the number of members in the ring, and that one of these fold configurations
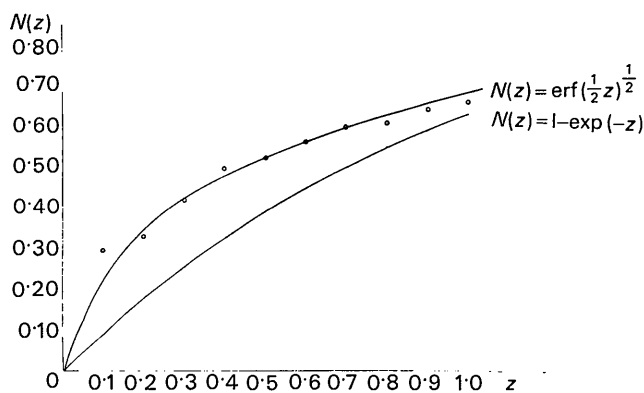

Fig.1. Distribution of intensities for the 0*kl* reflexions. $z =$ intensity expressed as a fraction of local average intensity. $N(z) = $ fraction of reflexions with intensity less than z.

* Present address: Department of Mechanics, Rutgers – The State University, New Brunswick, New Jersey, U.S.A.